Düzce University
Journal of Science & Technology

Experimental and Theoretical Study on Behaviour of Geometrically Asymmetric Composite Marine Sandwich Beams under Bending Load

Fatih BALIKOĞLU[a,*], Tayfur Kerem DEMİRCİOĞLU [a]

[a] *Department of Mechanical Engineering, Faculty of Engineering, Balıkesir University, Balıkesir, TURKEY*
* *Corresponding author's e-mail address: fatih.balikoglu@balikesir.edu.tr*
DOI.10.29130/dubited.1007940

ABSTRACT

This study presents a detailed investigation on the three-point and four-point bending behaviour of asymmetric sandwich beams composed of polyvinyl chloride (PVC) foam core and E-glass fibre reinforced polymer face sheets. The effects of mid-plane asymmetry on the bending load-displacement behaviour and failure mechanism of the sandwich beams were examined. Simple analytical expressions accounting for flexural and shear rigidities of the sandwich beams were proposed to predict the failure load, mid-span deflection and equivalent bending stiffness of the specimens and validated against experimental results. By shifting the loading direction, the flexural behaviour of asymmetric beams may be controlled. On the loading side, the use of face sheet with thick or high in-plane mechanical characteristics resulted in a delay in compressive failure of the top face sheet. The effective bending stiffness was overestimated since the applied formula did not account for shear deformations. First-order shear deformation theory was used to estimate the mid-span displacement values of sandwich beams in elastic regime and showed good agreement with the experimental results.

Keywords: Asymmetric sandwich beams, Flexural properties, PVC foam

Geometrik Olarak Asimetrik Kompozit Sandviç Kirişlerin Eğilme Yükü Altındaki Davranışı Üzerine Deneysel ve Teorik Çalışma

ÖZ

Bu çalışma, polivinil klorür (PVC) köpük çekirdek ve E-cam elyaf takviyeli polimer tabakalardan oluşan asimetrik sandviç kirişlerin üç nokta ve dört nokta eğilme davranışları hakkında ayrıntılı bir araştırma sunmaktadır. Sandviç kirişlerin eğilme yükü-sehim davranışı ve hasar mekanizması üzerindeki orta düzlem asimetrisinin etkileri incelenmiştir. Sandviç kirişlerin eğilme ve kayma rijitlik değerlerini hesaba katan basit analitik ifadeler, numunelerin hasar yükünü, kiriş orta-nokta sehmini ve eşdeğer eğilme rijitliğini tahmin etmek için önerilmiş ve deneysel sonuçlar ile doğrulanmıştır. Yükleme yönünü değiştirerek, asimetrik kirişlerin eğilme davranışı kontrol edilebilir. Yükleme tarafında, kalın veya yüksek düzlem içi mekanik özelliklere sahip yüzey tabakasının kullanılması, üst yüzey tabakasında basma hasarı gecikmesine neden olmuştur. Uygulanan formül kayma deformasyonlarını hesaba katmadığı için etkin eğilme rijitliği değerleri yüksek tahmin edilmiştir. Birinci mertebe kayma deformasyon teorisi, elastik bölgede sandviç kirişlerin orta açıklık deplasman değerlerinin tahmin etmek için kullanılmış ve deneysel sonuçlarla iyi bir uyum göstermiştir.

Anahtar Kelimeler: Asimetrik sandviç kirişler, Eğilme özellikleri, PVC köpük

I. INTRODUCTION

Sandwich composites are multi-layered materials made by gluing two strong, stiff, thin face sheets to a softer, lighter, thicker core. The core helps to stabilize the facings and provides flexural stiffness, out-of-plane shear, and compressive strength, while the face sheets carry almost all the axial and bending loads [1]. Such materials are extensively used in maritime applications due to their superior specific bending properties [2]. In addition, composite sandwich panels are an excellent choice for the marine industry because of their simple production, lightness (buoyancy), and resistance to the rough marine environment [3-5]. Glass, carbon, and Kevlar fibre reinforced laminates are commonly utilized as face sheets in maritime sandwich structures, whereas balsa wood and closed-cell polyvinyl chloride (PVC) are commonly used as core materials [6, 7]. Asymmetric sandwich structures have advantages in boat building, such as improving exterior impact and resistance to thermal/wear durability with a thicker outside face sheet while allowing connections with other structural components with a thinner interior face sheet [8].

Sandwich structures are typically exposed to flexural loads when used in boat hull constructions [9]. Therefore, much effort has been devoted on studying the behaviour of sandwich beams under bending loads using experimental, theoretical, and finite element methods [10-25]. In the literature, first order shear theory was successfully applied to estimate the experimental deflections in the linear region of a sandwich beam with two stiff face sheets and a soft core [24]. Theoretical calculations using the mechanical properties of the components obtained from the coupon tests, on the other hand, deviated from the estimation of the actual failure loads. This difference was due to the combined effect of shear and bending stresses on the sandwich beams and the non-linearity of the component materials [12,13]. In addition, the predicted bending stiffness values of the sandwich beams were found to be higher than the effective stiffnesses due to the soft foam core material with low shear modulus causing large shear deformation [25].

Previous efforts have concentrated on the bending behaviour and failure modes of symmetric sandwich beams, and there is limited documented literature on asymmetric sandwich beams subjected to in-plane and bending loads [26-36]. The mid-plane asymmetry may reduce the bending curvature caused by service loads, which introduces bending stresses into the face sheet in addition to in-plane membrane loads, increasing the risk of buckling of the compression face sheet [27]. The failure mechanism and bending strength of asymmetric beams varies according to loading direction, face sheet and core thickness and material properties [31-33]. The experimental and numerical responses of such asymmetric sandwich panels loaded under combined compression and shear forces were evaluated. In terms of core deformation and the continuity of normal and shear stress throughout the thickness, the predictions on strain distributions matched experimental results well [29, 34]. Asymmetric sandwich panels with tapering and junction sections are also usually applied in practical applications. The tapered region has a major impact on the stability and load-bearing capacity. This increased the asymmetry by introducing additional bending moments into sandwich panels, resulting in early local buckling [35].

The present paper deals with the three and four-point bending behaviour of asymmetric beams. The effect of mid-plane asymmetry on the flexural behaviour of the asymmetric sandwich beams was investigated. Simple theoretical formulations were used to predict the failure load, stiffness, and mid-span displacement of the asymmetric beams.

II. MATERIAL AND METHODS

A. MATERIALS

Sandwich specimens made of E-glass reinforced polymer face sheets and 25 mm thick Airex C70.75 closed cell PVC foam with a density of 80 kg/m^3 [37]. As reinforcement materials for the face sheets, E-glass non-crimp biaxial stitched fabrics with areal weights of 850 g/m^2 and 600 g/m^2 were used. For this research, two different asymmetric beams were designed. As seen in Table 1, the asymmetric geometry was obtained in the first specimen by applying a different layer number of 850 gr/m^2 fabric, and in the second specimen by using fabrics with different areal weights of 850 gr/m^2 and 600 gr/m^2. The mechanical characteristics of the face sheets were measured by testing the coupon specimens to relevant ISO [38] and ASTM [39, 40] test standards (Table 2). As matrix material, an infusion type vinyl ester resin (Poliya 702) was used [41].

B. PRODUCTION OF COMPOSITE SANDWICH PANELS

Resin infusion method was applied to manufacture sandwich composite panels. Figure 1 shows the components of VARIM (vacuum assisted resin infusion moulding) production schematically. E-glass fabrics and PVC foam were placed in the mould in a dry form according to the stacking sequence, and a vacuum bag was placed on top of the mould (Fig. 2 a), which was initially connected to a resin supply and a vacuum pump. In the resin system, 2 wt. % methyl ethyl ketone peroxide (MEKP) as initiator and 0.25 wt. % cobalt naphtanate (CoNap) as accelerator was added before the infusion process. The liquid resin penetrated the reinforcement materials as a result of the vacuum drawn through the mould at 1 atm negative pressure, (Fig.2 b) and then curing and demoulding processes were applied at room temperature. Test specimens were cut from the panels with in-plane dimensions of 500 mm × 80 mm (total length (L_t) × width (b)) [42] (Fig. 3 a, b). The panels were cured at room temperature for 24 hrs. following the infusion process. Specimens ASB_1 and ASB_2 had mid-plane asymmetry because of different numbers of E-glass fabrics and fabric weight in the face sheet laminates, respectively. Details of asymmetric beams are given in Table 1.
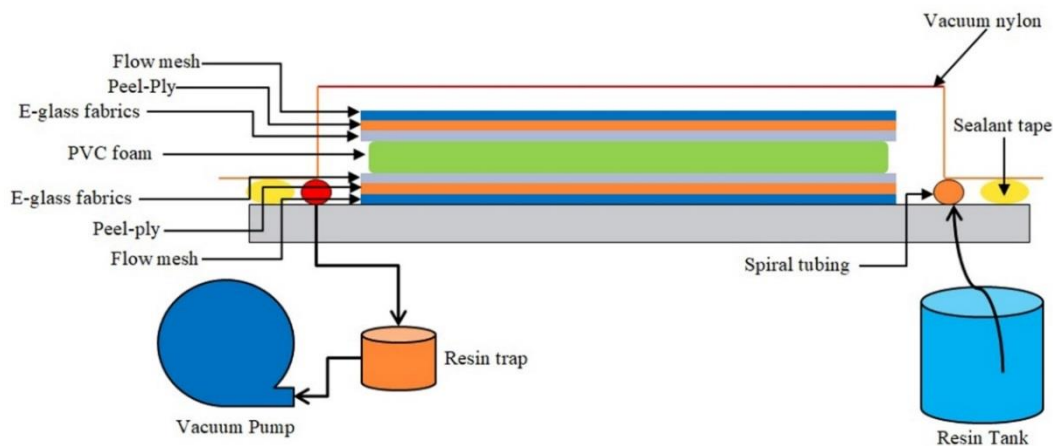

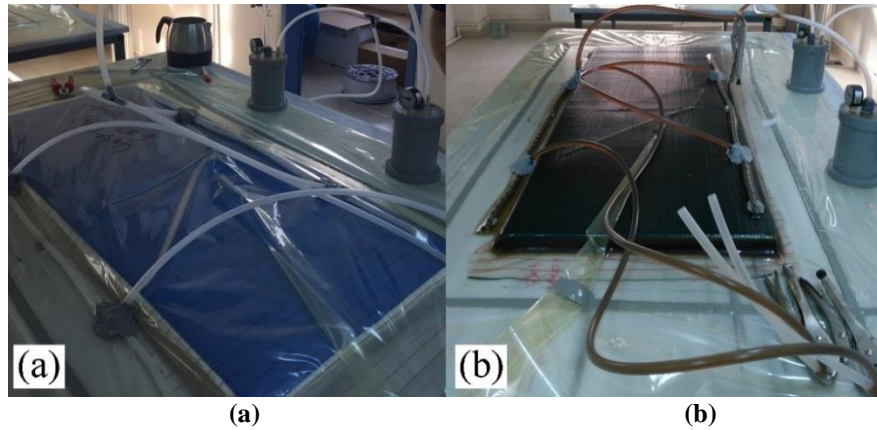*Figure 1.* *Schematic of resin infusion process.*

(a) **(b)**

Figure 2. *Production of sandwich panels with resin infusion method (**a**) dry, (**b**) wetted panel.*
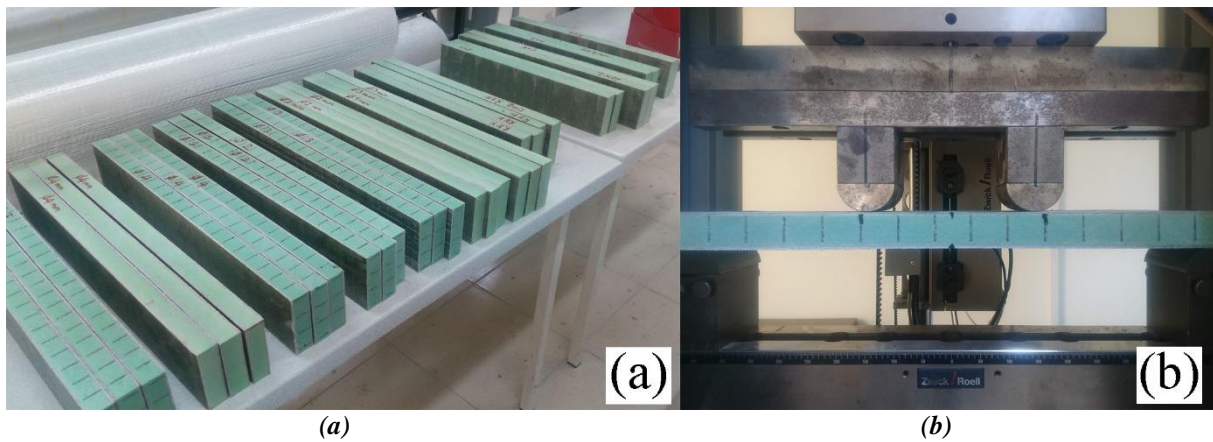

(a) *(b)*

Figure 3. *Sandwich test specimens (**a**), undeformed test specimen before 4-point bending test (**b**).*

Table 1. *Details of asymmetric sandwich beams.*

Specimens	Face sheet	Stacking Sequences	Areal weights (kg/m^2)	Face sheet thickness (mm)	e* (mm)	Beam Width (mm)	Total thickness (mm)
ASB$_1$	Up	$[0/90]_{3s}$	850	4.0±0.1	17.45	80±0.8	31.5±0.2
	Down	$[0/90]_{2s}$	850	2.5±0.1	10.8	80±0.8	
ASB$_2$	Up	$[0/90]_{2s}$	850	2.5±0.1	11.15	80±0.8	29.5±0.2
	Down	$[0/90]_{2s}$	600	2.0±.0.1	16.1	80±0.8	

*e= distance between neutral axis and centroid of the lower face sheet

C. TEST SET-UP

Three-point bending (3PB) and four-point bending (4PB) tests were performed according to ASTM C393 / C393M-16 standard [43]. Since the face sheets are not geometrically symmetrical, asymmetric sandwich beams were subjected to flexural-up and flexural-down tests, as used by researchers [8, 30]. For the flexural-up tests (see Fig.4a, b), the thicker face sheet was loaded at the top surface of the beams, and at the flexural-down tests (see Fig.4c, d), the thicker face sheet was loaded at the bottom surface of the beams [30]. To minimize local indentation damage beneath the loading points and supports each had a diameter of 25 mm. The tests were performed at a constant loading rate of 6 mm/min. The support span length (L) was 450 mm at the three-point and four-point bending tests. The loading and shear spans were 1/3 of the support span (L) in four-point bending tests. For each

sandwich beam type, at least three examples were prepared and loaded in the warp direction. All beams were loaded to collapse to determine the failure load and damage modes. To identify the specimens, a specific coding system was applied. The abbreviations ASB_1 and ASB_2 represent two different asymmetric sandwich beams 1 and 2. ASB_2-$TS_{450,\,up}$, for example, refers to an ASB_2 specimen with a span length of 450 mm subjected to 3PB flexural up loading. ASB_1-$FS_{450,\,down}$ represents an ASB_1 specimen with a span length of 450 mm subjected to 4PB flexural down load.
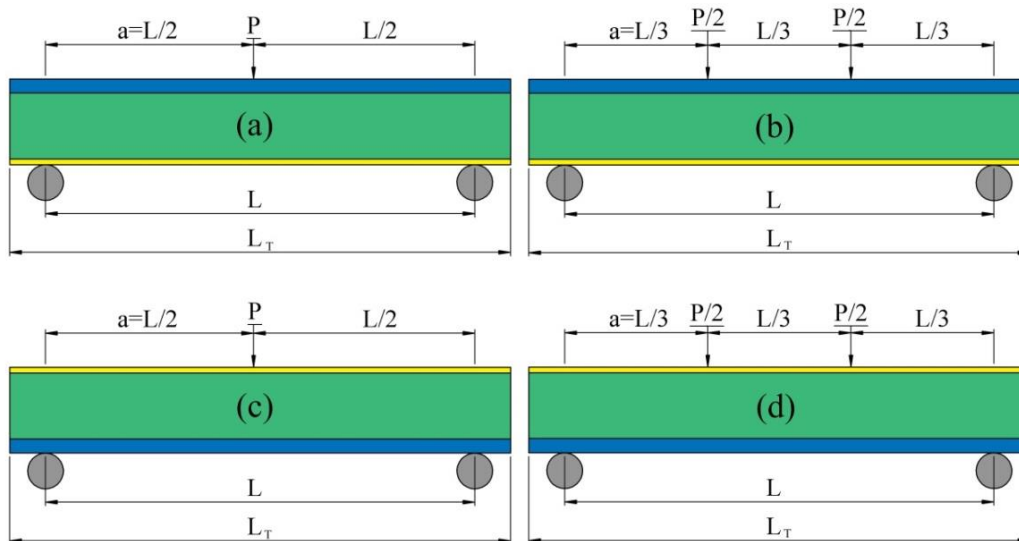

Figure 4. *Test typology, (a) 3PB flexural-up test set-up, (b) 4PB flexural-up test set-up, (c) 3PB flexural-down test set-up, (d) 4PB flexural-down test set-up, P=applied load, L=support span length, L_T=total span length, a=shear span.*

Table 2. *Mechanical characteristics of face sheets in warp direction.*

| Test | Areal weight (g/m²) | 850 | | 600 | | 850 | |
	Stacking Sequence	[0/90]₂ₛ		[0/90]₂ₛ		[0/90]₃ₛ	
	Values	**Average**	**S.D***	**Average**	**S.D***	**Average**	**S.D***
Tensile [38]	Modulus *(GPa)*	22.5	0.42	19.2	0.39	22.9	0.43
	Strength (MPa)	332	19.25	312	9.66	347	8.47
	Maximum strain *(%)*	1.89	0.8	2.0	0.16	1.92	0.03
Compression [39]	Modulus *(GPa)*	32.7	1.55	22.2	0.60	32.9	1.49
	Strength *(MPa)*	176	20.03	92.2	4.15	180	19.16
Shear [40]	Modulus *(GPa)*	4.14	0.18	3.30	0.10	4.49	0.19
	Strength *(MPa)*	52.9	1.9	39.6	0.60	55.6	1.8

*S.D: Standard deviation

III. ANALYTICAL STUDY

A. ESTIMATION OF EQUIVALENT BENDING AND SHEAR STIFFNESS FOR ASYMMETRIC SANDWICH BEAMS

The cross-sectional geometry of symmetric and asymmetric sandwich structures is shown in Figure 5 (a) and (b), respectively.
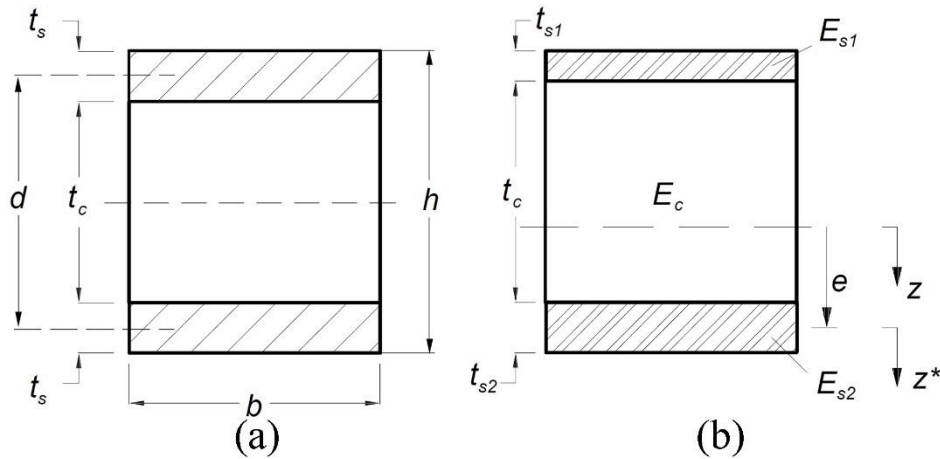
Figure 5. *The cross-sectional geometry of the symmetric (**a**) and asymmetric (**b**) sandwich composite beams.*

Equivalent bending stiffness ($EI_{eq., sym.}$) of the symmetric beams can be obtained using the sum of the flexural stiffness of the face sheet and core about the centroid axis of the cross-section [44].

$$EI_{eq.sym.} = E_s \frac{bt_s d^2}{2} + E_s \frac{bt_s{}^3}{6} + E_c \frac{bt_c{}^3}{12} \tag{1}$$

where E_c and E_s are the Young's modulus of PVC foam and the E-glass reinforced polymer face sheet material, respectively.

For asymmetric beams, firstly the location of the neutral axis must be assigned. It is provided by the coordinate system for which the first moment of area is zero when integrated across whole cross-section. Since the location of the origin of the sought coordinate system is unknown, make a coordinate transformation from a known point in the section, e.g. $z* = z - e$, according to Fig. 5 (b).

$$B(z) = \int Ezdz = \int E(z^* + e)dz^* = 0 \rightarrow -\int Ez^* dz^* = e \int Edz^* \tag{2}$$

where $B(z)$ is the first moment of area.

For an asymmetric sandwich cross-section as shown in Fig.5 (b), this equation can be re-written as Eq. (3) [1]:

$$E_{s1}t_{s1}\left(\frac{t_{s1}}{2} + t_c + \frac{t_{s2}}{2}\right) + E_c t_c \left(\frac{t_c}{2} + \frac{t_{s2}}{2}\right) = e(E_{s1}t_{s1} + E_c t_c + E_{s2}t_{s2}) \tag{3}$$

where t_{s1} and t_{s2} are thicknesses, E_{s1} and E_{s2} are the Young's modulus of dissimilar face sheets.

$$e = \frac{E_{s1}t_{s1}\left(\frac{t_{s1}}{2} + t_c + \frac{t_{s2}}{2}\right) + E_c t_c \left(\frac{t_c}{2} + \frac{t_{s2}}{2}\right)}{E_{s1}t_{s1} + E_c t_c + E_{s2}t_{s2}} \tag{4}$$

where e is the distance between the centroid of the lower face sheet (t_{s2}, E_{s2}) and the neutral axis as shown in Fig. 5 (b).

$$d - e = \frac{E_{s2}t_{s2}\left(\frac{t_{s2}}{2} + t_c + \frac{t_{s1}}{2}\right) + E_c t_c \left(\frac{t_c}{2} + \frac{t_{s1}}{2}\right)}{E_{s1}t_{s1} + E_c t_c + E_{s2}t_{s2}} \tag{5}$$

For the ASB$_1$ beam, this e value for the flexural down and up positions was calculated as 10.8 mm and 17.45 mm, respectively. In the ASB$_2$ beam, the e value was found to be 11.15 mm and 16.1 mm for flexural down and up, respectively.

The bending stiffness of the asymmetric specimens can be determined using Eq. (6) [1] by using the parallel axis theorem:

$$EI_{eq,asym.} = E_{s1}\frac{bt_{s1}^3}{12} + E_{s2}\frac{bt_{s2}^3}{12} + E_c\frac{bt_c^3}{12} + E_{s1}bt_{s1}(d-e)^2 + E_{s2}bt_{s2}e^2 + E_cbt_c\left(\frac{t_{c}+t_{s2}}{2}-e\right)^2 \tag{6}$$

where d=t_{s1}/2+t_c+t_{s2}/2 is distance between centroids of the skins.

The shear stiffness of asymmetry (AG_{eq}) sandwich beams can be defined by Eq. (7) [44]:

$$AG_{eq} = bdG_c \tag{7}$$

where b refers the beam width and G$_c$ represents the shear modulus of PVC foam material [37].

B. ESTIMATION OF FAILURE LOADS AND MECHANISMS

The material and test parameters such as sample dimensions, mechanical properties and test typology (loading action and direction) can all affect the failure load and mechanism of sandwich beams. For expressions of equations, the detailed cross-sectional sizes of the sandwich composite beams are given in Fig. 5.

The shear failure in the core depends on the shear strength of the foam material [45]. Eqs. (8, 9) represent the core shear failure load (Ps) [1]:

$$P_S = \frac{2(EI_{eq})\tau_c}{E_{s1}t_{s1}(d-e) + \frac{E_c}{2}\left[-d+e+\frac{t_{s1}}{2}\right]^2} \qquad -d + e + \frac{t_{s1}}{2} \le x \le 0 \tag{8}$$

$$P_S = \frac{2(EI_{eq})\tau_c}{E_{s2}t_{s2}e + \frac{E_c}{2}\left[e-\frac{t_{s2}}{2}\right]^2} \qquad 0 \le x \le e - \frac{t_{s2}}{2} \tag{9}$$

where τ$_c$ is the shear strength of PVC foam.
In-plane damage was caused when the compressive stress of the outermost fibres of the face sheet under bending load exceeds its compressive strength. The predicted failure load (P$_b$) of asymmetric beams can be determined by Eqs. (10, 11) [46]:

$$P_b = \frac{\sigma_c(EI_{eq})}{CE_{S1}L(d-e+\frac{t_{s1}}{2})} \tag{10}$$

$$P_b = \frac{\sigma_c(EI_{eq})}{CE_{S2}L(e+\frac{t_{s2}}{2})} \tag{11}$$

where L is the total span length, σ$_c$ is the strength of E-glass reinforced polymer face sheets under compression load. C is applied as 1/6 for the third-point loading (L/3) at four-point bending test and as 1/4 for the three-point bending test.

C. ESTIMATION OF MID-SPAN DEFLECTION

For beams under 3PB and 4PB tests as illustrated in Fig. 4, according to the first order shear deformation theory, the mid-span deflection is the total of the bending ($\delta_{bending}$) and shear (δ_{shear}) deformation of the beam:

$$\delta_{total,3PB} = \delta_{bending} + \delta_{shear} = \frac{PL^3}{48EI_{eq}} + \frac{PL}{4AG_{eq}} \qquad \text{for three-point bending tests} \qquad (12)$$

$$\delta_{total,4PB} = \delta_{bending} + \delta_{shear} = \frac{23PL^3}{1296EI_{eq}} + \frac{PL}{6AG_{eq}} \qquad \text{for four-point bending tests} \qquad (13)$$

where L is the total span length, P is the applied load. The detailed equivalent bending (EI_{eq}) and shear (AG_{eq}) stiffness calculations are given in Section III.A.

D. ESTIMATION OF STIFFNESS

Equations (14) and (15) give the bending stiffness values of sandwich beams.

$$K_i = \left[\frac{\Delta P}{\Delta \delta}\right] \quad \text{initial bending stiffness} \qquad (14)$$

$$EI_{eff} = \frac{a(3L^2 - 4a^2)}{48}K_i \quad \text{effective bending stiffness} \qquad (15)$$

where ($\Delta P/\Delta \delta$) represents the slope of the actual load–displacement graphs in linear elastic portion. L is the support span length and a is the shear span, denoting the distance between the support and loading points.

IV. RESULTS AND DISCUSSION

A. LOAD-DISPLACEMENT CURVES

Load versus crosshead displacement curves of the sandwich specimens tested under 3PB and 4PB tests are shown in Figures 6 and 8. The test results of all the beams are summarized in Table 3, including the ultimate bending strength (P_u), ultimate bending strength to weight ratio (P_u/W), analytical to experimental ultimate bending strength ratio (P_a/P_u) and failure modes.

The 3PB flexural down and up test results of the ASB_1 specimen are shown in Fig. 6 a, b. Compressive failure of the top face sheet was dominant for ASB_1-$TS_{450,down}$ and ASB_1-$TS_{450,up}$ specimens due to bending effect (see Fig. 7 a, b). Moreover, the displacement values at failure were almost doubled in the 3PB flexural-up tests. This result confirmed previous studies, that face fracture was delayed with increasing thickness of the top face sheet [36]. In 4PB tests, ASB_1-$FS_{450,down}$ and ASB_1-$FS_{450,up}$ specimens exhibited similar failure loads and also the same damage modes (Fig. 8 a, b). The ultimate bending strength of ASB_1 specimen tested at the 3PB flexural up load was 10.1% greater than that of flexural down. M. E. Toygar et al. [32] reported that the ultimate bending loads were higher in three-point bending flexural up tests compared to flexural down. The thicker outer face sheet could distribute local loads more uniformly, enhancing the sectional stability and ultimate bending strength of the specimens. Similarly, increasing the top face thickness of asymmetric beams increased their load-bearing capacity, according to the literature [36].

The 3PB flexural down and up test results of the ASB_2 specimens are shown in Figs. 6 c, d. The upper face sheet fibre failure was dominant in 3PB tests associated with higher loads under flexural up loading (see Fig.7 c, d). The ultimate bending strength of the ASB_2-$TS_{450, up}$ specimens was 30.5% greater than that of ASB_2-$TS_{450, down}$ counterparts. The thinner top face sheet under flexural down tests caused a poor performance due to premature compressive failure of the face sheet [8]. This finding revealed that the face fracture of the sandwich sample with a thin top face sheet occurred easily [36]. At this point, it should be noted that the top face sheet was not only thinner but also lower in in-plane properties was effective. Furthermore, the distance from the neutral axis increased the bending stress in flexural down tests. This may contribute to early face sheet failure under the loading point. ASB_2-$TS_{450,up}$ specimens sustained almost two times the displacement at failure in comparison to the ASB_2-$TS_{450,down}$ specimens (Fig. 6 c, d). For the ASB_2-$FS_{450, down}$ specimen, a sudden load drop occurred after a short non-linear region due to face sheet compression failure (Fig. 8 c). The load-displacement curves for the ASB_2-$FS_{450,up}$ specimen were nearly linear until shear cracks formed in PVC foam. After the linear part of the curves, the slopes dropped significantly, resulting in a non-linear action up to the shear failure in PVC foam. Debonding damage took place between face sheets and foam, as shown in Fig. 8 d.
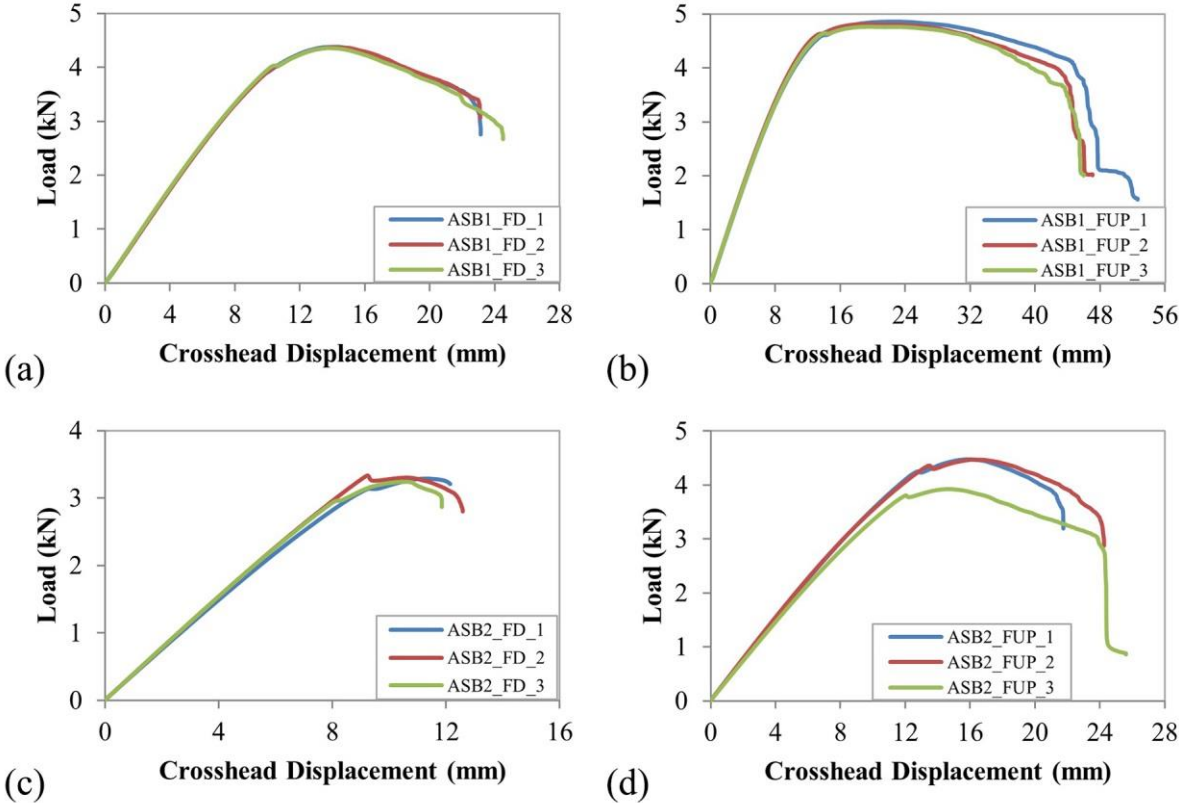

Figure 6: *Load-crosshead displacement curves of ASB_1 and ASB_2 specimens tested under 3PB test, (a) ASB_1-$TS_{450, down}$, (b) ASB_1-$TS_{450, up}$, (c) ASB_2-$TS_{450, down}$, (d) ASB_2-$TS_{450, up}$.*

Table 3. Summary of bending test results.

Specimens	P_u (kN)	P_u/W (kN/kg)	P_a/P_u	Failure Modes
ASB_1-$TS_{450,up}$	4.809	7.18	1.425	FC
ASB_1-$TS_{450,down}$	4.367	6.52	1.290	FC
ASB_1-$FS_{450,up}$	5.861	8.75	0.923	CS+D
ASB_1-$FS_{450,down}$	5.883	8.78	0.930	CS+D
ASB_2-$TS_{450,up}$	4.291	8.96	1.008	FC
ASB_2-$TS_{450,down}$	3.288	6.86	1.092	FC
ASB_2-$FS_{450,up}$	5.114	10.68	1.016	CS+D
ASB_2-$FS_{450,down}$	4.767	9.95	1.114	FC

Note: P_u: Experimental ultimate bending strength; **P_u/W:** experimental ultimate bending strength to weight ratio; **P_a/P_u:** analytical to experimental ultimate bending strength ratio; **CS:** Core shear failure; **FC:** Face compression failure; **D:** Debonding
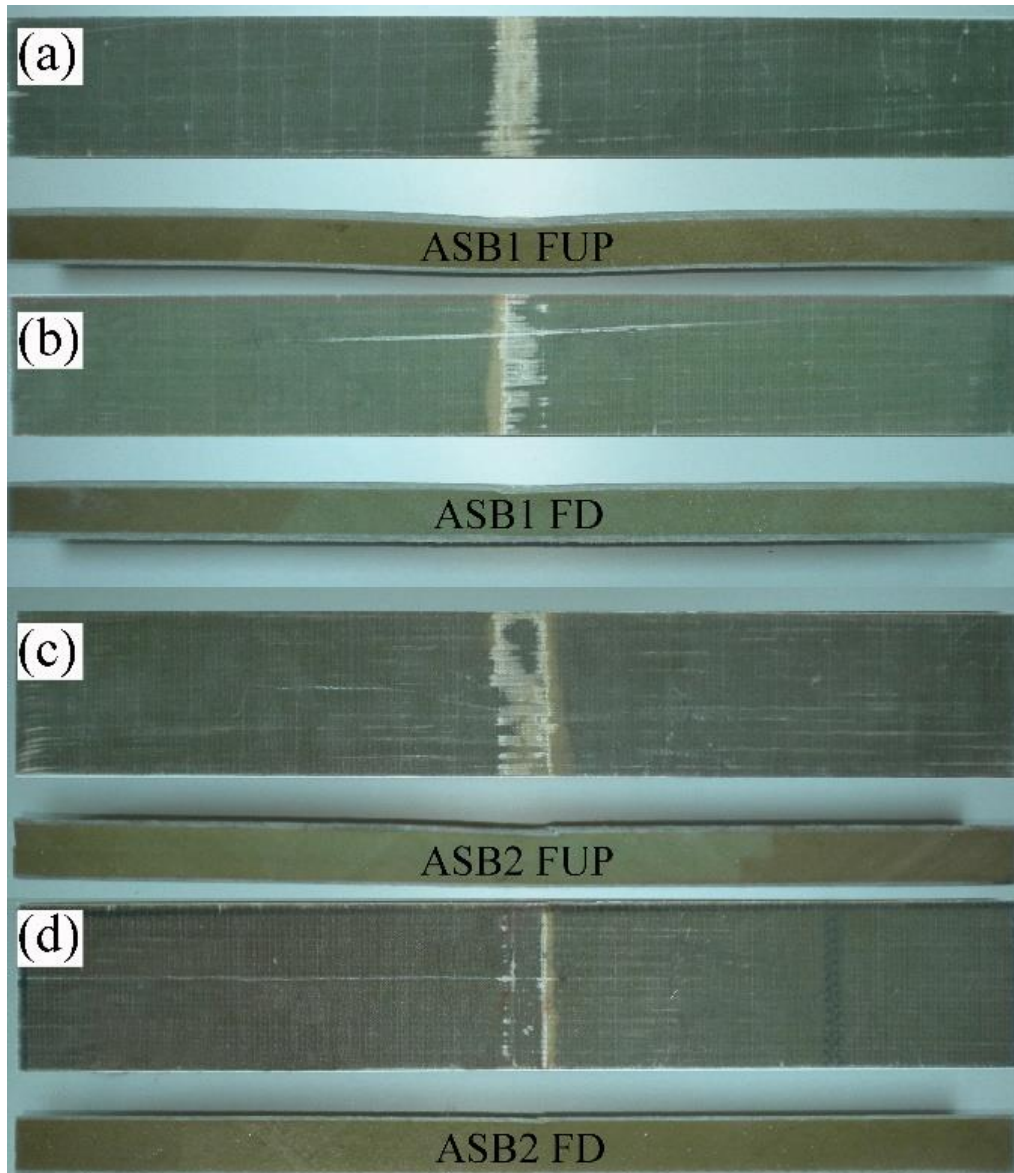

Figure 7. Damage photos of ASB_1 and ASB_2 specimens tested under 3PB test, (a) ASB_1-$TS_{450, up}$, (b) ASB_1-$TS_{450, down}$, (c) ASB_2-$TS_{450, up}$, (d) ASB_2-$TS_{450, down}$.
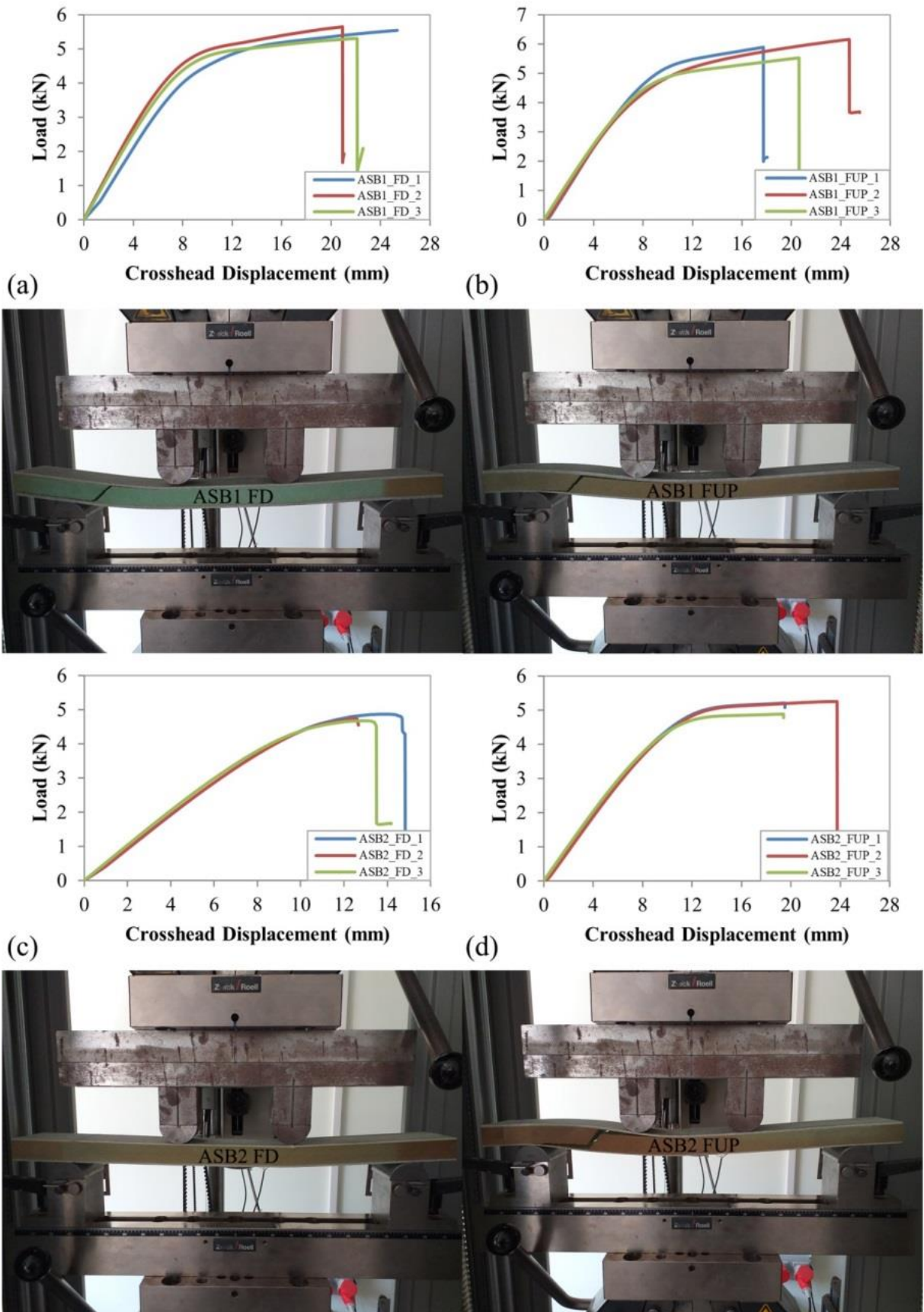
Figure 8. *Load-crosshead displacement curves of ASB₁ and ASB₂ specimens tested under 4PB test and damage photos, (a) ASB₁-FS₄₅₀, down, (b) ASB₁-FS₄₅₀, up, (c) ASB₂-FS₄₅₀, down, (d) ASB₂-FS₄₅₀, up.*

B. FAILURE LOADS

The results for asymmetry beams showed that the difference between the theoretical loads based on Equations (8), (9), (10) and (11) actual failure loads ranges from 0.8% to 42.5%. This underestimation between the theoretical and experimental failure loads may be attributed to the material properties used in the analytical equations and also the complex state of stress between loading point and top face sheet where the failure initiated could not be accounted for in the proposed analytical equations [47]. Table 3 also shows a comparison between the specific ultimate bending loads of the specimens (P_u/W). These specific strength values are based on the individual weights of the sandwich beams after production. The asymmetric beams ASB_1 and ASB_2 weights are 14.4 and 10.3 kg/m^2, respectively.

C. MID-SPAN DISPLACEMENTS

Table 4 shows the theoretical (th.) and experimental (exp.) deflections collected from the linear-elastic zone at 1 kN and 2 kN. Figure 9 shows the change in shear and bending deflection contributions for 3PB and 4PB tests. The bending and shear effects are equal in case of flexural up and down loads. For 4PB tests, it was observed that the bending contribution reached the highest value for ASB_1 and ASB_2 beams. The total displacement formula for asymmetry beams overestimated the mid-span displacement by 1.6% on average, with a standard deviation of 0.09. The first-order shear deformation theory gave results in agreement with the experimental displacements in the elastic regime of the sandwich beams. This was due to the assumption of linear elastic behaviour of the component materials in the analytical model [24]. The difference between theoretical and experimental displacements ranges from 0.09 mm to 0.503 mm. It can also be seen that in general, in flexural down tests, this difference tends to be higher (Table 4). This could be due to the presence of the thicker face sheet in the bottom side. This resulted in a higher resistance of the sandwich beams at flexural-down loading in elastic region.

Table 4. *Comparison of analytical and experimental mid-span displacements of asymmetric sandwich beams.*

Specimens	Load (kN)	$\delta_{b.th.}$ (mm)	$\delta_{s.th.}$ (mm)	$\delta_{tot.th.}$ (mm)	$\delta_{exp.}$ (mm)	$\delta_{tot.th.}/\delta_{exp.}$
ASB_1-$TS_{450,up}$	1 kN	0.844	1.488	2.332	2.14	1.090
	2 kN	1.689	2.976	4.665	4.32	1.080
ASB_1-$TS_{450,down}$	1 kN	0.844	1.488	2.332	2.08	1.121
	2 kN	1.689	2.976	4.665	4.25	1.098
ASB_1-$FS_{450,up}$	1 kN	0.719	0.992	1.711	1.89	0.905
	2 kN	1.439	1.984	3.423	3.79	0.903
ASB_1-$FS_{450,down}$	1 kN	0.719	0.992	1.711	1.88	0.910
	2 kN	1.439	1.984	3.423	3.72	0.920
ASB_2-$TS_{450,up}$	1 kN	1.387	1.589	2.976	2.7	1.102
	2 kN	2.775	3.178	5.953	5.49	1.084
ASB_2-$TS_{450,down}$	1 kN	1.387	1.589	2.976	2.62	1.136
	2 kN	2.775	3.178	5.953	5.45	1.092
ASB_2-$FS_{450,up}$	1 kN	1.182	1.059	2.241	2.36	0.950
	2 kN	2.364	2.119	4.482	4.74	0.946
ASB_2-$FS_{450,down}$	1 kN	1.182	1.059	2.241	2.34	0.958
	2 kN	2.364	2.119	4.482	4.7	0.954
Results						
Ave.	-	-	-	-	-	1.016
SD	-	-	-	-	-	0.09

Note: $\delta_{b,th.}$: theoretical bending deflection; $\delta_{s,th.}$: theoretical shear deflection; $\delta_{tot.th.}$: total theoretical deflection; δ_{exp}: total experimental deflection.
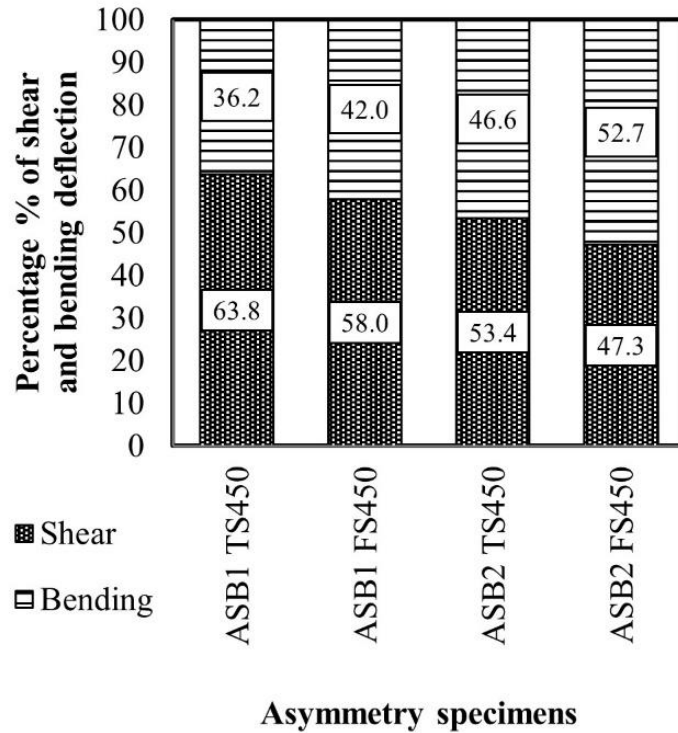
Figure 9. Bending and shear contributions to mid-span deflection values

D. BENDING STIFFNESS

The bending stiffness values of the sandwich beams are summarized in Table 5. ASB_1 beams had greater effective bending stiffness values in comparison with the ASB_2 specimens. This result suggested that the increase in the moment of inertia and stiffer face sheet material made a more marked contribution to theoretical stiffness of the specimens. For the 4PB tests, the effective bending stiffness of the ASB_1 and ASB_2 beams had the highest values. A deviation in the range of 0.08-2.27% was observed in the bending stiffness results due to flexural up and down loads. The outer thicker face sheet above or below the central core further to the neutral axis of the cross-section could give maximum advantage to the bending stiffness of the beams [48]. Comparing the experimental and analytical bending stiffness values, shear deformations reduced the composite action of the sandwich cross-section during the experiments, resulting in lower effective bending stiffness compared to equivalent bending stiffness (Table 5) [49].

Table 5. Bending stiffness values of asymmetric sandwich beams.

Specimens	K_i (kN/mm)	$EI_{eff.}$ (10^6 N.mm^2)	$E_{eq.}/E_{eff.}$	$EI_{eff.}/W$ (N.mm^2/kg)
ASB_1-$TS_{450,up}$	0.44	835.6	2.690	58.0
ASB_1-$TS_{450,down}$	0.439	834.9	2.693	57.9
ASB_1-$FS_{450,up}$	0.672	1086.2	2.070	75.4
ASB_1-$FS_{450,down}$	0.657	1062	2.117	73.8
ASB_2-$TS_{450,up}$	0.389	739.4	1.850	71.8
ASB_2-$TS_{450,down}$	0.392	744	1.839	72.2
ASB_2-$FS_{450,up}$	0.521	842	1.625	81.7
ASB_2-$FS_{450,down}$	0.525	848.3	1.613	82.4

V. CONCLUSIONS

In this study, the flexural behaviour of asymmetric sandwich beams was evaluated using three-point and four-point bending test methods and simple analytical expressions.

- The test results revealed that the flexural behaviour of asymmetric beams may be manipulated by changing the loading direction.
- The use of the weaker face sheet in asymmetry beam caused the damage to be governed by the failure of the face sheet under compression.
- The thicker face sheet can offer a large bending stiffness to composite beams; therefore, the ultimate bending strength can be improved by increasing the outer face sheet thickness.
- Asymmetry sandwich beams could be used in the flexural up position in order to resist higher bending loads.
- The parallel axis theorem and sandwich beam theory were used to derive the formulae for calculating the equivalent and effective bending stiffness values.
- The applied formula did not account for shear deformations, resulting in an overestimation of effective bending stiffness.
- Analytical model based on the first-order shear deformation theory to predict the mid-span deflections of the specimens showed a good agreement with the experimental results.
- The use of thicker face sheet resulted in an increase in the equivalent bending stiffness values, thus a decrease in the bending effect, while the use of a face sheet with lower in-plane mechanical properties caused an increase in the bending deflection values.

V. REFERENCES

[1] Zenkert, D., "Chapter 3: Fundamentals" in *An Introduction to Sandwich Structures*, Chamelon, Oxford, 1995, pp. 3.1-3.12.

[2] A. Mouritz and R. Thomson, "Compression, flexure and shear properties of a sandwich composite containing defects," *Composite structures,* vol. 44, no. 4, pp. 263-278, 1999.

[3] L. Calabrese, G. Di Bella, and V. Fiore, "Manufacture of marine composite sandwich structures," in *Marine Applications of Advanced Fibre-Reinforced Composites*: Elsevier, 2016, pp. 57-78.

[4] D. Zenkert, "Damage tolerance of naval sandwich panels," in *Major Accomplishments in Composite Materials and Sandwich Structures*: Springer, 2009, pp. 279-303.

[5] L. Sutherland, "A review of impact testing on marine composite materials: Part III-Damage tolerance and durability," *Composite structures,* vol. 188, pp. 512-518, 2018.

[6] A. Mouritz, E. Gellert, P. Burchill, and K. Challis, "Review of advanced composite structures for naval ships and submarines," *Composite structures,* vol. 53, no. 1, pp. 21-42, 2001.

[7] E. Greene. (2020, May 27). *"Lecture Notes." Eric Greene Associates, Inc.* [Online]. Available:http://ericgreeneassociates.com/webbinstitute.html.

[8] G. Di Bella, C. Borsellino, and L. Calabrese, "Effects of manufacturing procedure on unsymmetrical sandwich structures under static load conditions," *Materials & Design,* vol. 35, pp. 457-466, 2012.

[9]   J. Dai and H. T. Hahn, "Flexural behavior of sandwich beams fabricated by vacuum-assisted resin transfer molding," *Composite Structures,* vol. 61, no. 3, pp. 247-253, 2003.

[10]   T. Sharaf, W. Shawkat, and A. Fam, "Structural performance of sandwich wall panels with different foam core densities in one-way bending," *Journal of Composite Materials,* vol. 44, no. 19, pp. 2249-2263, 2010.

[11]   R. Umer, E. Waggy, M. Haq, and A. Loos, "Experimental and numerical characterizations of flexural behavior of VARTM-infused composite sandwich structures," *Journal of Reinforced Plastics and Composites,* vol. 31, no. 2, pp. 67-76, 2012.

[12]   A. Mostafa, K. Shankar, and E. Morozov, "Experimental, theoretical and numerical investigation of the flexural behaviour of the composite sandwich panels with PVC foam core," *Applied Composite Materials,* vol. 21, no. 4, pp. 661-675, 2014.

[13]   A. Mostafa, K. Shankar, and E. Morozov, "Behaviour of PU-foam/glass-fibre composite sandwich panels under flexural static load," *Materials and Structures,* vol. 48, no. 5, pp. 1545-1559, 2015.

[14]   H. Mathieson and A. Fam, "In-plane bending and failure mechanism of sandwich beams with GFRP skins and soft polyurethane foam core," *Journal of Composites for Construction,* vol. 20, no. 1, pp. 04015020, 2015.

[15]   W. Ferdous, A. Manalo, and T. Aravinthan, "Effect of beam orientation on the static behaviour of phenolic core sandwich composites with different shear span-to-depth ratios," *Composite Structures,* vol. 168, pp. 292-304, 2017.

[16]   S. V. Iyer, R. Chatterjee, M. Ramya, E. Suresh, and K. Padmanabhan, "A Comparative study of the three point and four point bending behaviour of rigid foam core glass/epoxy face sheet sandwich composites," *Materials Today: Proceeding*, vol. 5, no. 5, pp. 12083-12090, 2018.

[17]   W. Ferdous, A. Manalo, T. Aravinthan, and A. Fam, "Flexural and shear behaviour of layered sandwich beams," *Construction and Building Materials,* vol. 173, pp. 429-442, 2018.

[18]   C. Kaboglu, L. Yu, I. Mohagheghian, B. R. Blackman, A. J. Kinloch, and J. P. Dear, "Effects of the core density on the quasi-static flexural and ballistic performance of fibre-composite skin/foam-core sandwich structures," *Journal of Materials Science*, vol. 53, no. 24, pp. 16393-16414, 2018.

[19]   F. Balıkoğlu, N. Arslan, T. Demircioğlu, O. İnal, M. Iren, and A. Ataş, "Improving four-point bending performance of marine composite sandwich beams by core modification," *Journal of Composite Materials*, vol. 54, no. 8, pp. 1049-1066, 2020.

[20]   F. Zhang, J. Xu, B. Esther, H. Lu, H. Fang, and W. Liu, "Effect of shear span-to-depth ratio on the mechanical behavior of composite sandwich beams with GFRP ribs and balsa wood core materials," *Thin-Walled Structures,* vol. 154, p. 106799, 2020.

[21]   Y. Gupta, A. Jacob, and A. Mohanty, "Effect of the core thickness on the flexural behaviour of polymer foam sandwich structures," *IOP SciNotes*, vol. 1, no. 2, p. 024404, 2020.

[22]   Ł. Pyrzowski and B. Sobczyk, "Local and global response of sandwich beams made of GFRP facings and PET foam core in three point bending test," *Composite Structures*, vol. 241, p. 112-122, 2020.

[23]   M. Kazemi, "Experimental analysis of sandwich composite beams under three-point bending with an emphasis on the layering effects of foam core," *Structures*, vol. 29: Elsevier, pp. 383-391, 2021.

[24]   A. Giordano, L. Mao, and F.-P. Chiang, "Full-field experimental analysis of a sandwich beam under bending and comparison with theories," *Composite Structures*, vol. 255, p. 112965, 2021.

[25]   W. Liu, F. Zhang, L. Wang, Y. Qi, D. Zhou, and B. Su, "Flexural performance of sandwich beams with lattice ribs and a functionally multilayered foam core," *Composite Structures*, vol. 152, pp. 704-711, 2016.

[26]   Y. Frostig, M. Baruch, O. Vilnay, and I. Sheinman, "Bending of nonsymmetric sandwich beams with transversely flexible core," *Journal of Engineering Mechanics,* vol. 117, no. 9, pp. 1931-1952, 1991.

[27]   N. R. Satapathy and J. R. Vinson, "Sandwich Beams With Mid-Plane Asymmetry Subjected To Lateral Loads Analysis And Optimization," Master of Mechanical Engineering Thesis, Univerisity of Delaware, 1999.

[28]   N. R. Satapathy and J. R. Vinson, "Sandwich beams with mid-plane asymmetry subjected to lateral loads," *Journal of Sandwich Structures & Materials,* vol. 2, no. 4, pp. 379-390, 2000.

[29]   B. Castanié, J.-J. Barrau, and J.-P. Jaouen, "Theoretical and experimental analysis of asymmetric sandwich structures," *Composite Structures,* vol. 55, no. 3, pp. 295-306, 2002.

[30]   G. Di Bella, L. Calabrese, and C. Borsellino, "Mechanical characterisation of a glass/polyester sandwich structure for marine applications," *Materials & Design,* vol. 42, pp. 486-494, 2012.

[31]   J. Zhang, Q. Qin, W. Ai, H. Li, and T. Wang, "The failure behavior of geometrically asymmetric metal foam core sandwich beams under three-point bending," *Journal of Applied Mechanics*, vol. 81, no. 7, 2014.

[32]   M. E. Toygar, K. F. Tee, F. K. Maleki, and A. C. Balaban, "Experimental, analytical and numerical study of mechanical properties and fracture energy for composite sandwich beams," *Journal of Sandwich Structures & Materials*, vol. 21, no. 3, pp. 1167-1189, 2019.

[33]   F. Balıkoğlu, T. K. Demircioğlu, M. Yıldız, N. Arslan, and A. Ataş, "Mechanical performance of marine sandwich composites subjected to flatwise compression and flexural loading: Effect of resin pins," *Journal of Sandwich Structures & Materials*, vol. 22, no. 6, pp. 2030-2048, 2020.

[34]   B. Castanié, J.-J. Barrau, J.-P. Jaouen, and S. Rivallant, "Combined shear/compression structural testing of asymmetric sandwich structures," *Experimental Mechanics,* vol. 44, no. 5, pp. 461-472, 2004.

[35]   J. Deng, A. Peng, W. Chen, G. Zhou, and X. Wang, "On stability and damage behavior of asymmetric sandwich panels under uniaxial compression," *Journal of Sandwich Structures & Materials*, vol. 23, no. 6, pp. 1870-1901, 2021.

[36]   W. Zhang, Q. Qin, J. Li, B. Su, and J. Zhang, "A comparison of structural collapse of fully clamped and simply supported hybrid composite sandwich beams with geometrically asymmetric face sheets," *Composites Part B: Engineering*, vol. 201, p. 108398, 2020.

[37]   Core Materials. (2021, October 2). *Datasheet for Airex C70 PVC Foam* [Online]. Available: https://www.3accorematerials.com/en/markets-and-products/airex-foam/airex-c70-pvc-foam.

[38]   *E. ISO, "527–4. Determination of tensile properties–Part 4: test conditions for isotropic and orthotropic fibre-reinforced plastic composites. European Standard," International Organization for Standardization,* 1997.

[39]   *ASTM Standard Test Method for Compressive Properties of Polymer Matrix Composite Materials Using a Combined Loading Compression (CLC) Test Fixture*, ASTM D6641 / D6641M, ASTM, West Conshohocken, PA, 2016.

[40]   *ASTM Standard Test Method for Shear Properties of Composite Materials by V-Notched Rail Shear Method*, ASTM D7078 / D7078M, ASTM, West Conshohocken, PA, Pennsylvania, USA, 2012.

[41]   Poliya. (2021, December 29). *Data sheet for cured Polives 702 Bisphenol-A epoxy Vinylester Resin.* [Online]. Available: https://www.poliya.com/tr/bisfenol-a-epoksi-bazli-vinilester-recineler.

[42]   K.-T. Hsiao and D. Heider, "Vacuum assisted resin transfer molding (VARTM) in polymer matrix composites," in *Manufacturing techniques for polymer matrix composites (PMCs)*: Elsevier, 2012, pp. 310-347.

[43]   *ASTM Standard Test Method for Core Shear Properties of Sandwich Constructions by Beam Flexure*, ASTM C393 / C393M-16, ASTM, West Conshohocken, PA, 2016.

[44]   C. A. Steeves and N. A. Fleck, "Collapse mechanisms of sandwich beams with composite faces and a foam core, loaded in three-point bending. Part I: analytical models and minimum weight design," *International Journal of Mechanical Sciences,* vol. 46, no. 4, pp. 561-583, 2004.

[45]   I. M. Daniel, E. E. Gdoutos, J. L. Abot, and K.-A. Wang, "Deformation and failure of composite sandwich structures," *Journal of Thermoplastic Composite Materials,* vol. 16, no. 4, pp. 345-364, 2003.

[46]   A. Manalo, T. Aravinthan, W. Karunasena, and M. Islam, "Flexural behaviour of structural fibre composite sandwich beams in flatwise and edgewise positions," *Composite Structures,* vol. 92, no. 4, pp. 984-995, 2010.

[47]   A. Manalo, "Behaviour of fibre composite sandwich structures under short and asymmetrical beam shear tests," *Composite Structures,* vol. 99, pp. 339-349, 2013.

[48]   Y. Qi, H. Fang, H. Shi, W. Liu, Y. Qi, and Y. Bai, "Bending performance of GFRP-wood sandwich beams with lattice-web reinforcement in flatwise and sidewise directions," *Construction and Building Materials,* vol. 156, pp. 532-545, 2017.

[49]   P. Sadeghian, D. Hristozov, and L. Wroblewski, "Experimental and analytical behavior of sandwich composite beams: Comparison of natural and synthetic materials," *Journal of Sandwich Structures & Materials*, vol. 20, no. 3, pp. 287-307, 2018.